CMLS, Cell. Mol. Life Sci. 56 (1999) 184–199
1420-682X/99/040184-16 $ 1.50 + 0.20/0

CMLS Cellular and Molecular Life Sciences

Three-dimensional structure of motor molecules

K. Hirose[a,*] and L. A. Amos[b]

[a]National Institute for Advanced Interdisciplinary Research, 1-1-4 Higashi, Tsukuba, Ibaraki 305-8562 (Japan), Fax + 81 298 54 3049, e-mail: khirose@nair.go.jp
[b]MRC Laboratory of Molecular Biology, Hills Road, Cambridge, CB2 2QH (UK), Fax + 44 1223 213556, e-mail: laa@mrc-lmb.cam.ac.uk

Abstract. Images, calculated from electron micrographs, show the three-dimensional structures of microtubules and tubulin sheets decorated stoichiometrically with motor protein molecules. Dimeric motor domains (heads) of kinesin and ncd, the kinesin-related protein that moves in the reverse direction, each appeared to bind to tubulin in the same way, by one of their two heads. The second heads show an interesting difference in position that seems to be related to the directions of movement of the two motors. X-ray crystallographic results showing the structures of kinesin and ncd to be very similar at atomic resolution, and homologous also to myosin, suggest that the two motor families may use mechanisms that have much in common. Nevertheless, myosins and kinesins differ kinetically. Also, whereas conformational changes in the myosin catalytic domain are amplified by a long lever arm that connects it to the stalk domain, kinesin and ncd do not appear to possess a structure with a similar function but may rely on biased diffusion in order to move along microtubules.

Key words. Kinesin; ncd; microtubules; tubulin; myosin; actin; cryo-electron microscopy.

Introduction

Kinesins and myosins are molecular motors that hydrolyse adenosine 5′-triphosphate (ATP) in order to translocate, respectively, on microtubules or actin filaments, while transporting a wide range of cellular components. In each case, the native molecules usually consist of one or two motor domains (heads) attached to some sort of tail that is thought to interact with the component being transported or to form filaments in the case of some myosins. The motor domains, prepared either by proteolytic digestion or by expressing truncated constructs, were shown to be sufficient for ATP hydrolysis, interaction with the track and force production [1, 2]. Force production and movement must be accompanied by structural changes in the motor domain-track complex. The most widely accepted hypothesis for the myosin mechanism is the swinging cross-bridge model, in which (a part of) the myosin changes its angle while attached to actin [3]. Relatively little is known about how kinesin-related proteins move.

* Corresponding author.

Microtubules and actin filaments have polar structures, with the end that grows faster during assembly being referred to as the plus end. Motor molecules detect the polarity of the track and move in a defined direction. All of the myosins so far found move towards the plus end of an actin filament, whereas some of the kinesin-related proteins, such as the *Drosophila* ncd (*non claret disjunctional*) protein, move along a microtubule in the opposite direction from conventional kinesin [4, 5].

In order to understand how these molecular motors move and how the direction of movement is determined, it is necessary to know how the structures of the motor-track complex change during the ATPase cycle. Structural studies of kinesin and ncd have progressed rapidly in the last 5 years. The three-dimensional (3-D) structures of kinesin and ncd motor domains complexed with tubulin, studied by electron microscopy, were first reported in 1995 [6–8], and the atomic structures of monomeric motor domains were solved by X-ray crystallography in 1996 [9, 10]. In this review, our main focus is on the structures of kinesin

and ncd, especially when bound to microtubules, in comparison with the structure of myosin bound to actin. We try to relate the structural information with the possible mechanisms of motility.

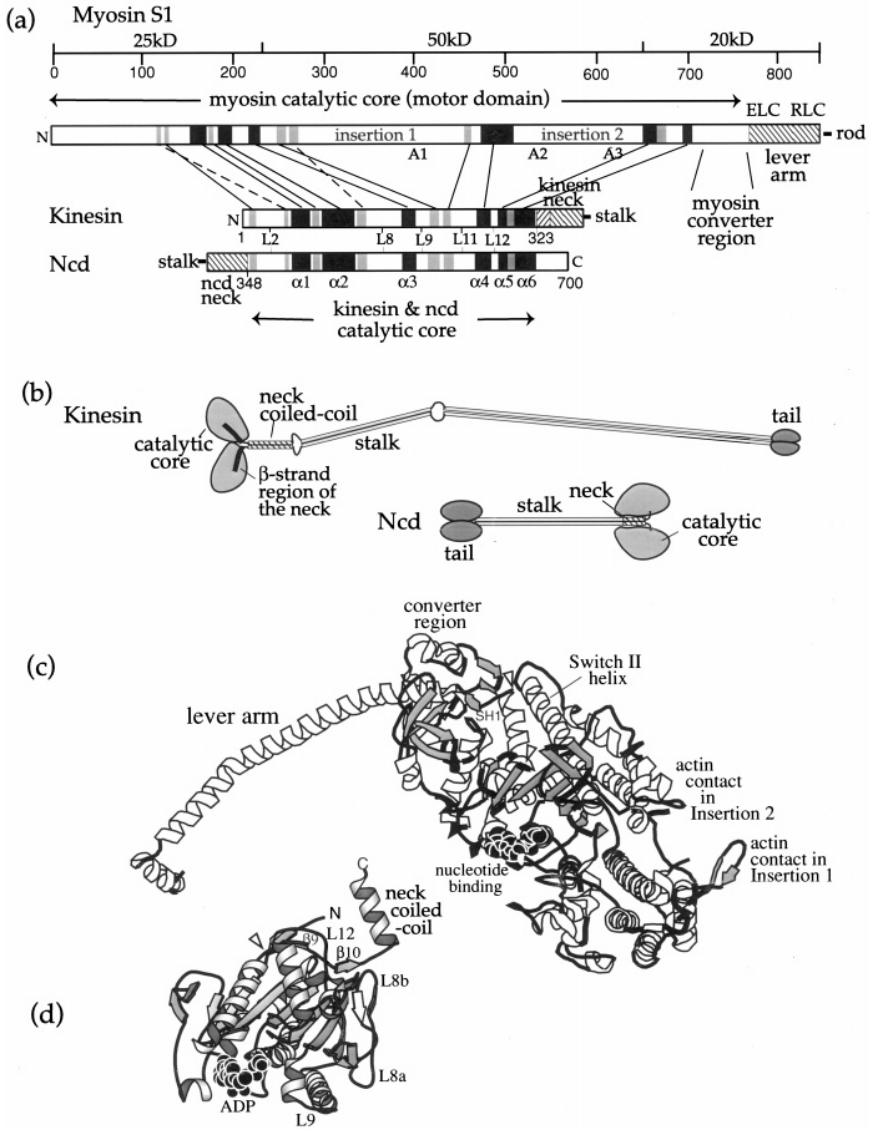

Figure 1. Structures of myosin S1 versus kinesin/ncd motor domains. (*a*) A schematic comparison of the amino acid sequences of the S1 fragment (motor domain plus long α-helical lever arm) of myosin and the motor domains of kinesin and ncd. α-Helical segments are shown in black, and β-sheet strands are shown in grey. Dimeric motors studied by electron microscopy (fig. 4b) include a short piece of coiled-coil, shown as a cross-hatched segment. The scale at the top shows amino acids in the myosin sequence numbered from the N-terminus. The 25-, 50- and 20-kDa fragments obtained by proteolysis are also marked. A1 (405–415), A2 (529–558) and A3 (626–647) label points in the myosin sequence that are believed to contact actin [72] and seem to be functionally equivalent to kinesin loops L8, L11 and L12, which probably contact tubulin. ELC and RLC refer to the essential and regulatory light chains of myosin II, which are associated with the lever arm (762–842). Adapted from [9]. (*b*) Molecular structures of whole kinesin and ncd heavy-chain dimers. In each case, the motor domains are connected via a coiled-coil stalk to a tail domain that interacts with the cargo. The difference is that kinesin's stalk and tail are at the C-termini of the motor domains; those of ncd connect to their N-termini. (*c*, *d*) Ribbon representations of the atomic structures of chicken myosin S1 heavy chain (modified from [18]) and kinesin motor domain [62]. This orientation shows a clear view of the relative positions of the nucleotides, the myosin loops that are thought to bind to F-actin and loops L8 and L12 of kinesin that are thought to bind face-on to microtubules. The arrowheads in (*c*) indicate the positions of the hinge points (Gly 699 and Gly 710) at each end of the SH1-containing helix that allow movement of the lever arm. The arrowhead in (*d*) indicates the start of the neck of kinesin that is thought to unpeel to allow the tethered catalytic domain more freedom to diffuse.

Structures of the kinesin and ncd molecules

Native molecules of conventional kinesin and ncd are homodimers (fig. 1b). Electron micrographs of rotary shadowed molecules show molecules with two more-or-less globular heads connected to a rodlike structure, supposed to be a coiled-coil [11, 12]. The head of kinesin corresponds to the N-terminal ~ 340 amino acids (aa), while the ncd head is at the C-terminus (fig. 1a). The head contains the nucleotide-binding and track-binding sites. The word 'motor domain', the domain that is sufficient for motility, is usually used to refer to the same part as the head, although there is no universal definition in either case (reviewed in [13]). Recently, the name catalytic core (or catalytic domain or motor core) is often used for a 320–330-aa part of a motor domain where the amino acid sequence is conserved throughout the kinesin superfamily ([13, 14]; see fig. 1). Beyond the catalytic core, there is a region called the neck, where the sequence is conserved only within certain kinesin classes [14]. For example, the catalytic cores of kinesin and ncd are similar, with $\sim 40\%$ amino acid identity, but the necks are different.

Recent studies have shown that both the position and sequence of the neck may be important in determining the directionality (see below). For movement towards the plus end, the precise sequence in some parts of the neck is less important. In vitro motility assays using multiple motors have shown that the 340-aa-long *Drosophila* kinesin construct (consisting of the catalytic core plus the start of the neck that contains two β-strands attached to an 11-aa flexible random chain can move microtubules at a velocity similar to that of the wild-type kinesin [15]. However, without the precise sequence in the β-strand region of the neck, the movement was extremely slow or not detected.

Motor mechanism and structure

Knowing about the structures of motor proteins is essential to understanding their mechanisms. They produce movement because local conformational changes at the ATPase active site are linked to other parts of the motor domains [3, 17, 18]. One set of linkages must connect the ATPase site to the tubulin or actin binding regions, affecting the binding affinity of the motor domain; this is because nucleotide turnover makes the motor cycle between weakly binding conformations, which readily detach from the track, and strongly binding conformations, which hold force. These linkages work reciprocally, in that the binding of tubulin or actin sends a signal in the reverse direction, altering the affinity of the active site for nucleotides and speeding up the process of product release. A second set of linkages connects to the tail domain, allowing conformational changes somewhere in the complex to pull on the load. These linkages also work reciprocally, so that tension on the motor molecule affects its affinity for nucleotides as well as for the track (the so-called Fenn effect) [19, 20]. To understand how the active site, the track binding and the load binding sites intercommunicate, it is essential to visualise the structures of the motor molecules and the way that they interact with subunits in the track.

Differences in the hydrolysis cycles of kinesin and myosin

Mg·ATP hydrolysis in both kinesins and myosins involves cleavage of the γ-phosphate bond followed by the release of phosphate (Pi) and subsequently of Mg·ADP (adenosine 5′-diphosphate). However, the transitions between weak and strong binding to their respective tracks, microtubules or actin filaments, occur at different points in the cycle. Myosin is unusual in that the products of hydrolysis ($Mg + ADP + Pi$) are all trapped in the active site if actin is not available for interaction [21]. Binding to actin causes the release of Pi, and the motor then locks strongly on to the track. In contrast, Pi is released from kinesin and ncd before re-binding to the track, but Mg·ADP remains trapped in the absence of microtubules [20, 22]. Microtubule binding triggers Mg·ADP release, which leads to strong binding.

2-D images of tubulin-motor complexes: polarity

When kinesin heads were first expressed in bacteria using recombinant DNA, several groups [2, 23, 24] showed that the heads can bind to microtubules with a periodic spacing of 8 nm, corresponding to the length of a tubulin heterodimer. This binding was visualised by 'negative stain' electron microscopy, in which the positions and shapes of protein molecules are revealed by the holes they occupy in a layer of heavy metal. Song et al. [25] also showed that the pattern of staining is characteristically polar; opened-out tubulin sheets (see fig. 3a) decorated with a monomeric construct of kinesin have bands of dark, light and intermediate density (fig. 2). It is possible to relate the orientation of the pattern to the plus and minus ends of microtubules by looking at brain tubulin sheets growing from the ends of microtubule 'seeds', such as pieces of flagellar axoneme or centrosomes isolated from tissue-culture cells. After some initial problems, results from different laboratories are now in agreement on this point (see [26–29]).

Images from unstained specimens in ice show reversed contrast compared with negatively stained specimens. Allowing for this difference, the two methods of speci-

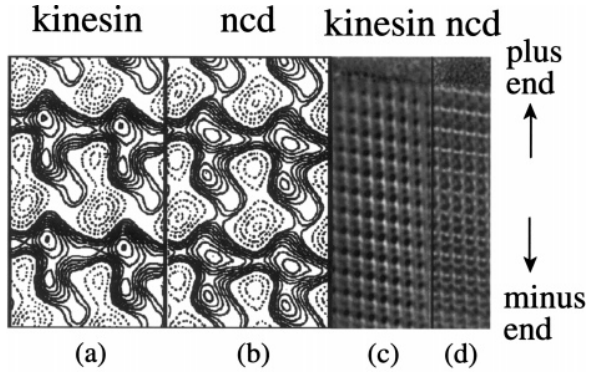

Figure 2. Kinesin and ncd bind to the same site on tubulin. Tubulin sheets decorated with motor domains and then negatively stained have an 8-nm repeating polar pattern, shown here as it appears with microtubule plus ends oriented towards the top of the page. (*a*, *b*) Comparison of high magnification images of sheets decorated with monomeric motor domains, obtained by computer analysis of many sheets (adapted from [28]): solid contours represent higher protein density; dashed contours include more stain and thus less protein. (*c*, *d*) Individual decorated sheets with visible ends (top of each figure), after computer enhancement of the periodic signal and filtering out of noise. Protein appears white here; surrounding stain is black ((*c*) adapted from [26], (*d*) from [6]). Whether the decoration is with kinesin or ncd, the pattern stops at the same stage at the end of the sheet, suggesting that kinesin and ncd bind in the same way to α- and β-tubulin.

men produce very similar results overall, except that stain gives particular emphasis to the top part of an attached motor domain, presumably because it excludes stain more completely. This leads to the lines of strong density running across the images in figure 2 [30].

One question addressed using electron microscopy is whether the opposite movements of kinesin and ncd could be explained in the way they bind to tubulin. However, the idea that ncd might move in the opposite direction to kinesin by binding to tubulin in the opposite orientation has been disproved fairly conclusively. The first indication was that tubulin sheets decorated with kinesin or ncd (fig. 2) show the same polarity [26, 28].

Both kinesin and ncd bind strongly to microtubules in the absence of nucleotides or in the presence of 5′-adenylylimidodiphosphate (AMP-PNP), a nonhydrolysable ATP analogue, but weakly when the nucleotide bound is ADP [31]. Both kinesin and ncd in all these three states were shown to bind in the same orientation, to equivalent sites on tubulin [6, 32]. The 3-D images referred to below (see fig. 4), showing motor molecules attached to microtubules or tubulin sheets [6–8, 33–37], also show kinesin and ncd heads to have very similar shapes and interactions with tubulin.

Methods for obtaining 3-D structures of tubulin-motor complexes

Since the electron microscope provides only projected views of 3-D objects, the structures of molecular complexes are not directly apparent. However, 3-D density maps can often be produced by computer processing of views from different angles. Because of the high background noise in electron microscope images, it is also essential to average data from many structural units.

In the presence of zinc ions, tubulin forms wide, well-ordered sheet structures, in which neighbouring protofilaments are antiparallel. Combining the micrographs taken by tilting these sheets through a variety of angles in the electron microscope, the 3-D structure of tubulin molecules has been successfully obtained at a high resolution [38]. Zinc sheets have not, however, been used to study the structure of motor-tubulin complexes, because it seems that kinesins bind only poorly to zinc sheets [39].

Three methods have been used to study the structures of motor molecules complexed with tubulin: helical reconstruction of symmetrical microtubules, 2-D crystal analysis using a tilted series of views of parallel tubulin sheets and back projection of twisted microtubules [40].

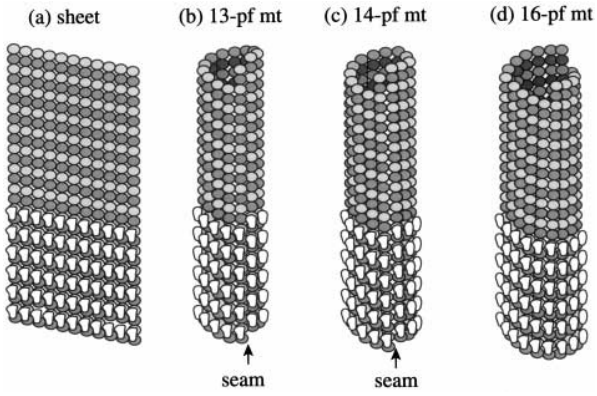

Figure 3. Various polymers of tubulin. All known tubulin polymers consist of polar arrangements of longitudinal protofilaments (pfs), each of which is a linear arrangement of $\alpha\beta$-tubulin heterodimers (represented here as a light monomer above a dark monomer). The lower dimers are shown decorated with monomeric motor domains (white). The tubulin sheet in (*a*) is essentially an opened-out microtubule (mt). Purified tubulin assembles mainly into the so-called B-lattice, in which heterodimers in adjacent protofilaments line up at a shallow angle. Most natural microtubules have 13 exactly longitudinal protofilaments, as in (*b*), but those assembled in vitro vary in pf number. Both the 13-pf (*b*) and 14-pf mts exhibit a 'seam' where lateral contacts are between light and dark subunits (the so-called A-lattice) rather than between like subunits. (*d*) Natural 16-protofilament microtubules (right) are apparently always seamless and, therefore, helically symmetrical, with two shallow dimer helices. In structures (*c*) and (*d*), the protofilaments twist very slowly around their tubes.

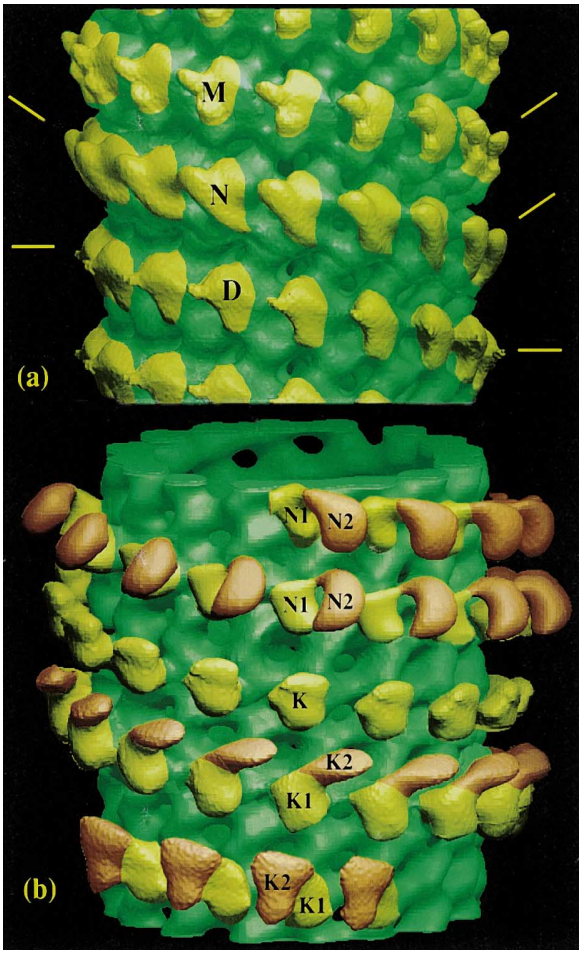

Figure 4. Comparison of different 3-D images of tubulin-motor-protein complexes. (*a*) Merged 3-D images of negatively stained 16-protofilament microtubules decorated with monomeric kinesin motor domains (adapted from [6]). Successive helical turns show results for different nucleotide conditions, and lines on either side indicate the change in tilt of a projecting feature, from roughly horizontal (ADP-bound state, kinesin head labeled D) to 45° (the nucleotide-free state, head labeled N and the AMP-PNP-occupied state, head labeled M). The difference in its position in the ADP-bound state, as compared with the other two states, is one indication of conformational changes between different nucleotide states. (*b*) Merged 3-D images of frozen-hydrated microtubules (adapted from [30, 33]). Parts of an undecorated microtubule (from [30]) are shown, together with images (from [32, 33, 77] of attached monomeric kinesin (K), dimeric kinesin (attached head K1, tethered head K2) and dimeric ncd (attached head N1, tethered head N2). The top and bottom rows of dimers are in nucleotide-free states, the three central rows of heads have bound AMP-PNP.

The number of protofilaments contained in a microtubule or a sheet used for all these studies is considerably less than that in zinc sheets. This results in a relatively low resolution (20–40 Å compared with <4 Å electron crystallography using zinc sheets). Nevertheless, the results provide valuable information about the structures of motor proteins interacting with tubulin.

Hoenger et al. [7] used tubulin sheets consisting of parallel protofilaments, which are opened-out microtubules (figs 2 and 3a), for studying the structure of motors bound to tubulin. The decorated sheets were flattened onto a carbon film by negative staining, to obtain 2-D crystalline arrays of the motor-tubulin complex. Reconstruction from negatively stained sheets provides relatively high resolution in the plane of the sheets, but lower resolution in the direction perpendicular to the lattice plane.

Helically twisted closed tubules do not require tilting since they present a 360° range of views of the repeating unit in a single image, and if the entire arrangement is helically symmetrical, information from many different subunits with a known relationship to each other can be readily combined. The helical reconstruction method has long been used to calculate 3-D structures of myosin-actin complexes [41–46]. Helical reconstruction of microtubules has been more difficult because most lack the required symmetry. Most of the microtubules occurring in vivo have 13 protofilaments (fig. 3b) which run exactly parallel to the microtubule axis and thus do not present a changing view of the structure. Microtubules polymerised from purified tubulin in vitro most commonly have 13 or 14 protofilaments, but some have fewer or more. If the protofilament number is not 13, then they follow a steeply sloping helical path [47], so that a single image of a microtubule has sets of tubulin subunits viewed from many angles.

The underlying arrangement of tubulin dimers is clearly revealed when microtubules are decorated with motor domains and tends to follow the so-called microtubule B-lattice [23], with dimers in adjacent protofilaments almost lined up. It was predicted that microtubules consisting of 11–15 protofilaments have a discontinuity ('seam'), where 2 neighbouring protofilaments have an A-lattice-like join (fig. 3b, c) [47]. The presence of such seams was confirmed by freeze-etching microtubules decorated with kinesin heads [48]. Microtubules with 10 or 16 protofilaments, on the other hand, were predicted to have true helical structures without seams, but such microtubules are unfortunately rare in normal preparations of reassembled pure tubulin. Kikkawa et al. [8] have calculated 3-D maps by analysing 10-protofilament microtubules in preparations of reassembled brain microtubules. Hirose et al. [6, 30, 33] used natural 16-protofilament microtubules that occur in the sperm tails of some insects [49], including crickets, for helical 3-D reconstruction.

A method using back projection was applied to twisted microtubules with and without seams [35, 50, 51]. The resulting images did not show very much detail, but the main value of this work was to show that an unexpected

proportion of the 15-protofilament microtubules reassembled from purified brain tubulin are helically symmetrical. Images of 15-protofilament microtubules are more easily obtained, because $\sim 10\%$ of the microtubules reassembled in the solution containing DMSO have 15 protofilaments [52]. Helical 15-protofilament microtubules have been used in recent studies of the 3-D structure of motor-microtubule complexes [32, 34, 36, 53].

3-D images of monomeric motors tightly bound to tubulin with AMP-PNP

3-D structures of monomeric kinesin heads complexed with tubulin in the presence of AMP-PNP, imaged by negative staining or ice embedding, have been reported by three different groups; 340–360 N-terminal residues of rat [6, 33, 53], mouse [8] and human kinesin heavy chain [28] all show similar conformations. The kinesin heads bind to the left half of the protofilament when the plus end is towards the top of the figure [26, 28] (see fig. 4).

A monomeric construct of ncd (366 C-terminal residues) bound to tubulin sheets showed a similar structure to kinesin heads [7, 37]. As already seen in 2-D images, ncd heads bind to equivalent sites on the tubulin dimer. This weighs further against models in which kinesin and ncd would move in opposite directions because they bind to tubulin with a different polarity or to different binding sites. Kinesin and ncd each seem to make contact with both α and β tubulin, as seen most clearly in cross-sections (e.g. [33]). This agrees with results from cross-linking studies [54, 55] and a blot overlay assay [56].

3-D images of dimeric motors tightly bound to tubulin with AMP-PNP

The two heads in a whole kinesin molecule are paired by coiled-coil segments at their carboxyl termini, whereas pairs of ncd heads are connected at their amino termini. Recombinant motor domains with a short coiled-coil segment can associate into dimers. It was reported that the N-terminal 365 residues of *Drosophila* kinesin heavy chain are predominantly monomeric and the constructs longer than 381 amino acids are predominantly dimeric [57].

Dimeric kinesin and ncd tightly bound to microtubules in the presence of AMP-PNP have been imaged in ice, and their 3-D structures calculated [33, 34, 36, 53]. Hirose et al. [33] and Arnal et al. [34] obtained quite similar results. In averaged maps of both kinesin and ncd dimers (see fig. 4b), only one of the two heads is directly attached to the microtubule, whereas the other head is tethered to the first head. Although the attached heads of dimers are essentially identical to attached monomeric heads, the unattached second heads emanate from slightly different points on the first heads and tilt in different directions; kinesin's second head lies closer to the plus end, whereas ncd's points towards the minus end.

The second heads of ncd in the images were as large as the attached heads and must have been tethered in a fixed position to appear like this. The second heads of kinesin, on the other hand, appear smaller, or even invisible in the maps calculated by some groups [53]. The reduced density of the second head in the averaged maps is likely to result from disorder of this head, because the second head is not directly attached to the microtubule, and connected only through a single amino acid chain in the neck unless there are extra associations between the head and neck or between the two heads. Another possible reason for the reduced density of the second head is that some of the dimers may bind with both heads to two tubulin dimers. Thormählen et al. [29] reported that tubulin sheets can be decorated with dimeric kinesin with a 16-nm banding periodicity, indicating that two heads of a kinesin dimer can bind to successive 8-nm-long tubulin dimers. But our results suggest that few molecules can be in this state when saturating levels of kinesin are mixed with microtubules.

Kinesin is thought to move along a microtubule using the two heads in a hand-over-hand fashion. Obviously, during the course of 'walking' along a microtubule, using the two heads alternately, a dimeric kinesin molecule should bind to a microtubule with both heads for a brief period, and then one of the heads should detach to search for the next binding site while the other is still attached. Thus, it is reasonable to expect two binding conformations: one with one head and the other with two heads. The proportion of these two conformations in the works described above must depend on the experimental conditions, such as the concentration of the proteins, or the timing in mixing kinesin, tubulin and nucleotides. There is also a disagreement about the binding stoichiometry of kinesin as measured by biochemical methods: the number of kinesin dimers that bind to a tubulin dimer ranges from 0.5 to 1 [24, 29, 31, 58, 59].

Hirose et al. [33] showed that the density levels of tethered heads in their images were significant by calculating difference maps comparing microtubules decorated with double-headed and single-headed motors. It is therefore fair to conclude that the images in figure 4b reveal an important structural difference between kinesin and ncd dimers.

Atomic structures of motors and tracks

The atomic structure of the myosin motor domain was first determined using chicken skeletal muscle myosin subfragment-1 (S1) without bound nucleotides [60]. The structure showed the N-terminal 770-aa catalytic core domain (see fig. 1) that contains the nucleotide binding and actin binding sites, connected to an 8.5-nm-long α-helical neck to which two light chains bind (fig. 1). It was suggested that the myosin neck works as a 'lever arm' that amplifies the small conformational changes within the catalytic core. Subsequently, the atomic structures of the myosin motor domains complexed with various nucleotides were solved (discussed below).

The motor domains of kinesin and ncd with bound ADP have also been studied by X-ray crystallography, and their 3-D structures solved to atomic resolution (see figs 5 and 6). Comparison of the catalytic cores of human kinesin and *Drosophila* ncd showed that these structures are closely similar [9, 10]. The central core of each structure consists of a seven- to eight-stranded β-sheet sandwiched between two sets of three α-helices; nucleotide binds to a site near one end of this structure during the active cycle. The similarity was probably not so surprising, considering that kinesin and ncd have high amino acid sequence similarity, but it left the question as to how these motors can move in opposite directions. Structural similarity in the catalytic core was also found in another minus end-directed kinesin-related protein, Kar3 [61].

Quite surprisingly, the 320-residue catalytic core domains of the kinesin family are also structurally related to the $\sim$700-residue motor domains of the myosin family, which have no apparent sequence similarity to kinesin [18]. These have essentially the same core structure (fig. 1c, d); only one β-strand within the cores of kinesin and ncd cannot be aligned with a similar feature in myosin. But the larger stretches of polypeptide that loop out from the myosin motor core are responsible for doubling its overall size compared with kinesin and ncd. These loops include segments that bind to actin or tubulin (see fig. 1). Despite the structural similarity within the catalytic core domains, the neck domains of myosin, kinesin and ncd were found to be very different: kinesin and ncd necks do not have a long α-helical lever arm as in myosin. The kinesin neck, visualised in the recent crystal structures of monomeric and dimeric rat kinesin motor domains [62, 63], consists of two β-strands (β9 and β10), and a segment of coiled-coil (figs 1b, d and 5; also see [64]). The neck of ncd, which is at the N-terminus of the catalytic core, has a coiled-coil structure, and is sandwiched between the two catalytic cores in the crystal structure of dimeric ncd (figs 1b and 6) [16]. Connected via different necks, the two heads of kinesin and ncd molecules are arranged in different ways: two kinesin

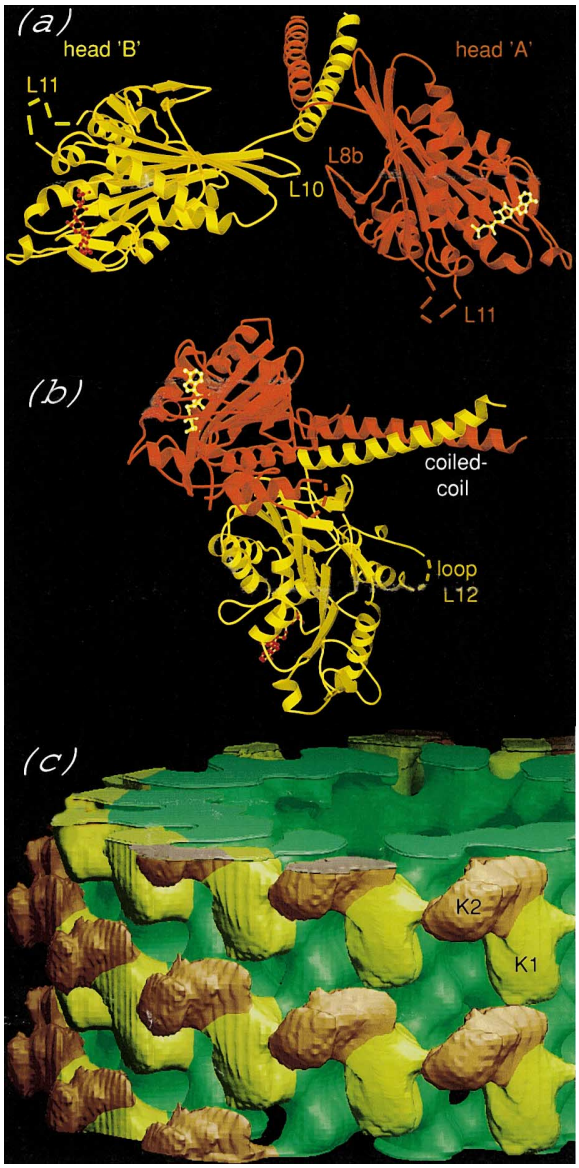

Figure 5. Dimeric kinesin motor domains at atomic and EM resolution. (*a*, *b*) Ribbon diagram of the crystallographic structure of dimeric rat kinesin [63]. (*a*) 120° rotation between the two heads. The heads make contact via loops L8b in head A and L10 in head B, as well as being bound together through the coiled-coil. The kinesin neck connecting the catalytic domain to the coiled-coil stalk is better seen in figure 1d. (*b*) The view from the front for the orientation with which we docked it into the map shown in (*c*), with head B as the directly attached motor domain. Bound ADP molecules are shown in contrasting colours. (*c*) 3-D image of a microtubule decorated with dimeric kinesin in the presence of ADP [77]. The directly attached (K1) and tethered (K2) heads are labeled for one kinesin dimer.

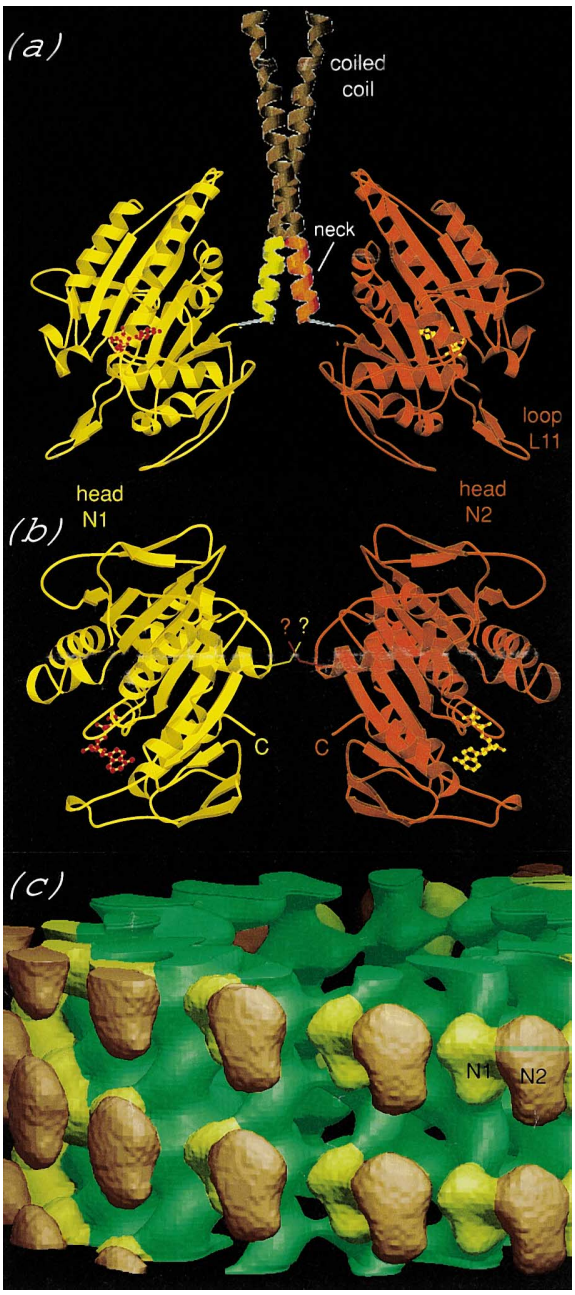

Figure 6. Dimeric ncd motor domains at atomic and EM resolution. (*a*) Ribbon diagram of dimeric ncd as in the crystal structure [16] with the two heads related about a twofold axis along the axis of the coiled-coil. In the crystal structure, the neck domains (shown coloured) at the N-termini of the ncd catalytic domains form a continuation of the coiled-coil stalk (see fig. 1), but this structure is probably unstable [16]. In (*b*) each head has been rotated so as to preserve a twofold relationship while bringing it into the orientation with which we docked it into the map shown in (*c*). Bound ADP molecules are shown in contrasting colours. (*c*) 3-D image of a microtubule decorated with dimeric ncd in the presence of ADP [32]. The directly attached (N1) and tethered (N2) heads are labeled for one ncd dimer.

heads are related by 120 degrees rotation, whereas the ncd dimer structure has a twofold symmetry (figs 5 and 6).

The structure of the tubulin dimers that make up microtubules has been determined at 3.7 Å resolution by electron microscopy of large 2-D crystals (electron crystallography) formed in the presence of zinc, and an atomic model has been fitted into it [38]. Since the crystals consist of protofilaments equivalent to those in microtubules, the structure shows the longitudinal interaction between tubulin heterodimers as well as that between monomers within a heterodimer. Each monomer consists of two globular domains, arranged on either side of a central α-helix, plus a C-terminal pair of helices that occupy a ridge on the protofilament surface. The N-terminal globular domains are homologous to the nucleotide binding domain of proteins like glyceraldehyde-3-phosphate dehydrogenase (GAPDH) which have a classical Rossmann fold [65] and bind guanosine 5′-triphosphate (GTP) in a pocket on the interface that contacts the next monomer along the protofilament.

The atomic structure of actin monomers has four roughly equal subdomains [66–69] and has no apparent relationship to tubulin, despite the similarities between myosin and kinesin. The structure of an actin filament was found by determining the orientation of G-actin monomers, arranged to form a filament, that gave best agreement with an X-ray pattern obtained from a gel of aligned actin filaments [70, 71].

Fitting of atomic structures into EM structures

In order to investigate the interactions between motors and tracks, the atomic structures have been fitted into 3-D density maps of motor-track complexes derived from cryo-electron micrographs. The atomic structures of myosin S1 and the actin monomer fitted into 3-D density maps of the actin-myosin complex [72, 73] showed separate regions of the motor domain interacting with two neighbouring actin monomers (see fig. 1).

For the microtubule motors, several groups have fitted the kinesin or ncd crystal structures into the EM maps of the motor-microtubule complex, but there is not yet a consensus for the orientation of the motors relative to tubulin. The reasons for the difficulty in determining the precise orientations are (i) the motors look relatively featureless at the current resolution of the EM maps; (ii) the atomic structures or the motors are known only for the ADP state, but it is difficult to obtain 3-D maps of motor-tubulin complexes in the weakly binding ADP state (described below).

Sosa et al. [36] and Hoenger et al. [53] docked monomeric ncd and kinesin crystal structures into EM maps of the motors strongly bound to microtubules in

the presence of AMP-PNP. The orientations chosen for the directly bound heads were similar and appeared to be in agreement with most of the data obtained by biochemical and mutagenesis studies [74–76]; both kinesin and ncd were oriented so that the loops, L8, L11 and L12, known to be involved in binding to tubulin, lay on the side facing the protofilament.

The crystal structures of dimeric kinesin and ncd were also fitted into the EM maps. Docking of the dimeric ncd crystal structure, with the bound head in the orientation described above, appeared to give a reasonable result [16], although the dimer would need to be greatly distorted in order to fit into the density in our 3-D maps (see fig. 6) [77]. The crystal structure of dimeric kinesin [63] could not be docked into EM density by Hoenger et al. [53] because their map was reported not to show any density corresponding to the unattached head. They suggested this was because the neck coiled-coil separated upon binding to a microtubule, and the two heads then bound to separate tubulin dimers. With one of the heads of the dimeric crystal structure docked into the density of the bound head in an orientation equivalent to the docking of ncd by Sosa et al. (1997), the neck coiled-coil pointed obliquely into the microtubule surface.

Kozielski et al. [78] and Hirose et al. [77] obtained EM maps of dimeric kinesin complexed to tubulin in the weakly bound, ADP state (see below), and used them for fitting the crystal structures of kinesin·ADP. For reasons that are not yet clear, the positions in these studies of the heads that are not directly bound are different, top-right of the bound head in Kozielski et al. and top-left in Hirose et al. when the plus end is towards the top of the picture (see below). Accordingly, the orientations chosen for fitting the kinesin structure are different. Both these orientations and that adopted by Sosa et al. and Hoenger et al. placed the point of the heart-shaped monomer, including L10 (see fig. 5a), at the top of the directly attached heads, but the disagreement occurs in the angle of rotation about the vertical axis.

The orientation chosen by Kozielski et al., with 'head A' of the crystal structure in the EM density of the bound head, has the neck coiled-coil pointing well away from the microtubule but has the drawback of placing the contact that kinesin makes with tubulin on the opposite surface from the studies described above, leaving the 'tubulin-binding' loops L11 and L12 on the exposed surface of the motor domain. To explain this, they suggested that kinesin might associate with microtubules via different surfaces at different stages in the motility cycle. Hirose et al. [77] placed 'head B' in the density of the bound head in their kinesin·ADP map and found the best fit in a different orientation. Although it was rotated by ~ 60 degrees compared with that chosen by Hoenger et al., the loops thought to be involved in tubulin binding still faced towards the microtubule, yet the coiled-coil segment was clear of the microtubule surface (see fig. 5b, c) [77].

Atomic coordinates for the $\alpha\beta$-tubulin heterodimer dock well into EM maps in a fairly unique orientation with the nucleotide binding site of β-tubulin at the faster-growing (plus) end. Lateral contacts between protofilaments involve a long hinged loop, which has been called the M loop [79], interacting with helix H3 on one side of the GTPase domain. This arrangement was first demonstrated in a 20-Å resolution EM map of an undecorated microtubule [79]; we have found the coordinates dock well in the same orientation into maps of decorated microtubules [Hirose et al., unpublished results]. Two long C-terminal helices, H11 and H12, in each tubulin monomer, occupy a ridge on the outside of a protofilament. The motor domains bind to a region that extends sideways between this ridge and helix H3 on the GTPase domains, while longitudinally the region is centered on the intradimer contact. Thus, the top half of a head interacts with the lower part of β-tubulin and the bottom half of the head with the upper part of α-tubulin.

Mutagenesis studies on kinesin [75] indicate that the residues important for interacting with tubulin are concentrated in a triangle defined by loops L8, L11 and L12, with the most crucial sequences being on L12 and the adjoining helix $\alpha 5$. This region interacts with β-tubulin. The interaction with α-tubulin may be weaker but appears to be important in the weakly binding ADP state [77]. The mutagenesis study also suggested that the entire interface is dominated by ionic interactions, in which positively charged groups on kinesin bind to negatively charged groups on the surface of tubulin.

The docking orientation of Sosa et al. and Hoenger et al. and the orientation that we favor [77] would both satisfy this prediction, putting the main contact surface on one side or the other of loop L11. The difference is that the first docking orientation would put L12 and $\alpha 5$ in direct contact with β-tubulin, even in the weakly binding ADP state. According to our results, there is a conformational change in the region of L12 and $\alpha 5$, in the transition from the ADP to the tightly bound states (see later). We predict that this change moves these crucial structures closer to tubulin and is responsible for the increase in binding affinity.

Conformational changes associated with nucleotide turnover in myosin

The original tilting cross-bridge model was proposed for myosin [80] soon after myosin cross-bridges were first observed between myosin thick filaments and actin-containing thin filaments, by electron microscopy of

muscle sections. There was, however, little evidence to support the model until recently. Attempts by electron microscopy to visualise a structural change have been repeatedly frustrated because it is difficult to saturate F-actin with S1 in the weak binding Mg·ADP·Pi initial attachment state and because molecules attach to actin at many different angles in the presence of ATP. More recent 3-D maps from cryo-EM images of smooth muscle and brush-border myosin heads bound to actin filaments [45, 46, 81] showed differences between the rigor (no nucleotide) and ADP-containing states: the bulk of the motor domain looked similar in both states, but the lever arm appeared to have rotated by 20–30 degrees as a consequence of losing bound ADP. The observed rotation corresponds to the 3–7 nm movement towards the plus (barbed) end of the actin filament. This was in agreement with the model in which the neck (light-chain binding region) of myosin works as a lever arm to produce movement of the molecule. However, the observed movement was associated with ADP release, not with phosphate release, which is thought to be the force-producing step. Also, no movement appears to occur in skeletal muscle myosin when Mg·ADP is released [82].

In the absence of actin, the structures of myosin heads complexed with various ADP and ATP analogs were studied at atomic resolution by X-ray crystallography. Crystal structures of the truncated *Dictyostelium* myosin heads (without the lever arm region) complexed with pyrophosphate, ADP·BeF_x (beryllium fluoride), ADP·AlF_4 (aluminium fluoride), ADP·Vi (vanadate), ATPγS, AMP-PNP or ADP [83–86; also reviewed in 3, 87–89] provide direct evidence for nucleotide-dependent conformational changes in myosin. The structures have been divided into two classes. The ADP·BeF_x, pyrophosphate, ATPγS and AMP-PNP complexes are thought to be analogues of a myosin·ATP state, and these structures are similar to each other. They are also similar to the ADP complex, and the original structure of chicken myosin that is without nucleotide but has sulfate in the active site. With ADP·AlF_4 and ADP·Vi, which are thought to mimic the transition states for nucleotide hydrolysis, there is a movement in the switch II element (Asp463-Glu 468 in chicken skeletal muscle myosin). This conformational change is accompanied by the partial closure of the large cleft in the 50-kDa domain (fig. 1), and a twist in the switch II helix (475–506 in chicken). The switch II helix runs from the active site to a so-called converter region (residues 711–767 in chicken). The twist in this helix results in a change in the two helices containing the reactive cysteine residues, SH1 (Cys 707) and SH2 (Cys 697), and the converter region. A rotation of approximately 70° around the glycine residue at the end of the SH1-containing helix is observed.

The converter region is followed by the α-helical lever arm region, though this region was not present in the truncated construct of the *Dictyostelium* myosin motor domain used for the crystallisation. Modeling the lever arm region into the *Dictyostelium* myosin structure with ADP·Vi showed that the C-terminal end of the lever arm could be rotated by as much as 12 nm compared with the chicken myosin structure without nucleotide [87]. Fitting these atomic structures into the EM maps of the myosin-actin complex showed that the movement of the tail with respect to actin is towards the minus (pointed) end of the actin filament during transition from the ADP·BeFx (ATP-like) to the ADP·Vi (transition state) structures, which are weakly bound states of myosin. Thus the lever arm is expected to swing back towards the plus (barbed) end to produce a 'power stroke' sometime during the product release.

Although it was a very attractive result, there was some uncertainty in this interpretation of movement of the lever arm, because considerable structural disorder was observed in the converter domain, which is at the C-terminus of the truncated *Dictyostelium* myosin, and also because presence of the light chains might affect the orientation of the converter region and the lever arm [85]. However, the recently reported structure of the smooth muscle myosin motor domain crystallised with the essential light chain ([90], also reviewed in [91]) showed that there is indeed a large angular change in the lever arm region. The converter region in the new crystal structure with ADP·AlF_4 was rotated by $\sim 70°$ compared with that in the chicken S1 structure. A comparison between the positions of the lever arm regions in these crystals showed that the C-terminal end of the lever arm may indeed be moved by ~ 12 nm.

We still have to keep in mind when interpreting these data that it is not totally clear how precisely crystal structures with nucleotide analogues mimic the real intermediate structures during the ATPase cycle, especially the structures when myosin is interacting with actin. Also, there could be more than one structural state corresponding to any one nucleotide state, and it is possible that only one of these conformations is stable enough to exist in a crystal. In fact, the structure of smooth muscle myosin with ADP·BeFx was very similar to the ADP·AlF_4 structure [90], whereas *Dictyostelium* myosin structure with ADP·BeFx was 'ATP-like', and similar to the nucleotide-free chicken S1 structure. It seems now clear, however, that there are at least two different myosin conformations and that the change from one to the other can produce a large motion in the C-terminal α-helical neck domain.

In solution, the movement may be even more dramatic than those seen in the crystal structures, since two cysteines known as SH1 and SH2, that can be cross-linked [92, 93] in the ADP·Vi state in solution (thereby

trapping ADP·Vi in the active site) are still 18 Å apart in the crystal structures, at opposite ends of a kinked α-helix between the active site and the lever arm. Intramolecular movement of the myosin motor domain in solution was also observed using fluorescence resonance energy transfer measurement [94]. The truncated *Dictyostelium* myosin motor domain was fused with green and blue fluorescent proteins at the N- and C-termini, respectively. The distance between the two fluorescent proteins changed in the presence and absence of various nucleotides.

There is additional evidence to support rotation of the lever arm. Uyeda et al. [95] made *Dictyostelium* myosin mutants with various lengths for the lever arm region, by deleting or adding extra light chain binding sites, and found that, up to a certain limit, the velocity of actin filament sliding is linearly related to the length of the neck. Similar results were obtained when the neck region was replaced by one or more repeats of α-actinin [96].

However, there are some experimental results that are difficult to explain by a simple 'lever-arm swinging' model. For example, the displacements, measured by some groups, that myosin can produce during a single interaction with an actin filament are too large (>20 nm) [97, 98] to be explained by a single power stroke of the 8.5-nm lever arm or by the transition between the two conformations observed in the crystal structures (~ 12 nm displacement). But other groups reported smaller values (~ 10 nm or smaller) [99, 100] that are consistent with the theory. Recent results measuring the displacement produced by a single myosin S1 attached to a scanning probe showed one to five substeps within a single displacement of 5–30 nm, which is probably produced utilising a single ATP molecule [98]. Each substep was ~ 5.3 nm, which is close to the distance of neighbouring actin molecules. If these results are true, how are they related to the two conformations seen in the crystals? We may have to reconsider the assumption that each structural state corresponds to a single biochemical or mechanical state.

Conformational changes in microtubule-motor complexes

Whereas the neck region of myosin consists of a long α-helix which is thought to work as a rigid lever arm, the atomic structures of kinesin and ncd show that their neck regions are unlikely to act as levers. Experiments showing that a monomeric 340-residue kinesin motor domain with an artificial flexible sequence attached to its C-terminus can still translocate microtubules [15] also make it unlikely that there is a lever arm outside the motor domain which is necessary for motility. If there are directed movements, they should occur within the motor domains (the catalytic core plus a part of the neck) and may be detectable by studying motor domains in different nucleotide states. However, kinesin and ncd are purified with an ADP molecule tightly bound to each head, and removal of ADP in the absence of microtubules causes denaturation of the motors [31]. All of the crystal structures of kinesin-related proteins so far obtained are in the ADP states, and there is as yet no crystallographic evidence for conformational changes in kinesin or ncd. However, conformational changes in the motor domains at different stages in the kinetic cycle are being studied by electron microscopy [6, 32, 77] (see figs 4–6).

As mentioned above, kinesin heads bind to the same position on the tubulin dimer, whether the nucleotide binding site of kinesin is empty or occupied. The 3-D images show subtle changes in the attached motor domain. The first evidence came from negatively stained images of monomeric kinesin (fig. 4a) in which a small protruding piece of structure (seen on the left side of the attached motors in fig. 4a) appeared to point in a direction at right angles to the microtubule axis in the ADP-bound state but was tilted towards the plus end in the nucleotide-free and AMP-PNP-occupied states. Maps of dimeric kinesin imaged in ice (figs 4b and 5) show more dramatic changes in the positions of the second heads, which probably amplify any changes in the attached heads.

In the absence of nucleotide, the tethered head of dimeric kinesin tilts downwards from its position in the ADP state (bottom row of fig. 4b compared with 5c). Thus, if the underlying top part of the attached head tilts upwards, the tethered head must rotate downwards about its point of attachment to the bound head. In the ATP-like (AMP-PNP) state, the tethered head of dimeric kinesin (second row from the bottom in fig. 4b) swings over to the right-hand side of the bound head, while the negatively stained image suggests that the pointed structure remains more or less in the same position as in the empty state. There is no evidence, therefore, that a large change in the attached head is responsible for moving the tethered head from one position to another. Thus, the largest movement that we see between different maps does not appear to be produced by any kind of leverage. An alternative model to account for the difference between the maps for the nucleotide-free and ATP-like states is for nucleotide-dependent conformational changes in the bound head to cause the tethered head to dissociate and reassociate with the bound head differently [101]. It is possible that, whereas the bound head corresponds to 'head B' and the tethered head to 'head A' in our maps of the ADP-filled (fig. 5) and empty (fig. 4b) states, the two heads may reverse their relationship in the ATP-like

state. It is also possible that there are other ways of interaction between the two heads or the head and the neck in these different nucleotide states, which may not be seen in the crystal structures of kinesin with ADP.

Kozielski et al. [78] have obtained a different structure for kinesin bound in the presence of ADP, with the tethered head close to the microtubule surface, to the top-right of the bound head. There may be two different stages in the kinetic cycle when kinesin·ADP is attached to the microtubule: one may occur soon after ATP hydrolysis, and the other after detaching and re-binding to the microtubule with ADP still bound (the 'initial' binding state). Upon binding to tubulin, ADP is released, and the motor settles down into the empty state. Our specimens were produced by decorating microtubules in the absence of nucleotide and by adding ADP just before freezing. It seems likely that the motor domains were then driven backwards into the 'initial' ADP state. The specimens of Kozielski et al., on the other hand, were incubated in a phosphate buffer with ADP for 5 min and may have been in a state similar to the ADP·Pi or ADP states that occur before detachment from tubulin. This difference may help us to understand the complete cycle of conformational movements.

Conformational changes in tubulin could also contribute to movement. However, although Hoenger et al. [7, 37] reported significant rearrangements in a microtubule when kinesin or ncd molecules bind to it, Hirose et al. [30] found only small changes. Both groups agree that the tubulin lattice parameters remain unchanged. Hirose et al. [6] also saw no obvious change in the tubulin lattice when varying the nucleotide state of kinesin. The only significant change seen in our maps is that the β-tubulin subunit tilts when kinesin or ncd is in a strongly bound state, compared with when they are weakly bound or absent [32, Hirose et al., unpublished results]. Nevertheless, it is possible that more significant transient changes occur during active movement.

The kinesin/ncd directionality problem

The motor domain of kinesin is at the N-terminus, whereas the ncd motor domain is at the C-terminus. So far, all the kinesin-related proteins that have the motor domain at the N-terminus move towards the plus end, whereas all the C-terminus motors with known directionality move towards the minus end (see Kinesin HomePage [105]). In 3-D images, as described above, while kinesin and ncd motor domains bound to tubulin are almost indistinguishable, the second, unattached heads of dimeric molecules are differently oriented (fig. 4b). The second head of a kinesin dimer, joined to the attached head at its C-terminus, is oriented towards the plus end in the presence of AMP-PNP, while the second head of ncd, joined at the N-terminus to its partner, points towards the minus end [33, 34]. Appropriate positioning of the free head by the bound head will clearly help to bias the direction in which the free head moves. However, it is not in itself enough to explain how kinesin and ncd move in opposite directions, because monomeric kinesins can move microtubules also.

Two heads of a dimeric motor are connected to each other through the neck (see figs 1, 5 and 6). Recent studies using chimaeric motors suggest that the direction of movement is determined by the neck region. The structures of the necks of kinesin and ncd are very different: the kinesin neck includes β-strands (β9 and β10; see fig. 1d), as well as a stretch of α-helix that makes a coiled-coil, and the ncd neck has an α-helical structure (see fig. 6) that is probably unstable. It has been suggested that conformational changes in the neck regions cause the motility of the motors in the opposite directions [16]. When the catalytic core of a dimeric construct of kinesin was exchanged with the ncd catalytic core, the chimaera motor moved towards the plus end, the direction of kinesin, suggesting that the directionality is determined in the region outside of the catalytic core [102, 103]. An opposite chimaera, a dimeric ncd construct but with the catalytic core from kinesin, moved in the direction of ncd [104]. However, when two residues in the neck of this latter chimaera, including the glycine residue at 347, were mutated, the construct moved in the kinesin direction, though very slowly. A dimeric ncd construct with the neck replaced by 12 random amino acids also moved towards the plus end [16]. These results suggest that the position of the motor domain does not in itself determine the direction of movement. The default direction of movement for the catalytic core is towards the plus end, and specific features of the neck are critical for the minus end-directed movement of ncd.

The processivity mechanism

Kinesin tracks microtubule protofilaments efficiently and in all probability moves 'hand over hand' in 8-nm steps along a single protofilament [15, 20, 106–109]. To do this, each motor domain needs to detach and swing forward 16 nm to its next binding site [20]. Quite clearly, this will require some kind of conformational change, probably in the neck region via which the two motor domains associate. A model in which part of the α-helical coiled-coil reversibly unravels [58] was suggested, since it is predicted that some residues there are not ideal for a stable coiled-coil [110, 111]. However, dimeric kinesin constructs in which most of the neck coiled-coil was deleted or replaced by a stable coiled-

coil were still able to move processively, although the distances they moved were shorter than the wild type [112]. Thus, unzipping of the neck coiled-coil is not essential for processivity of kinesin, but may help. An alternative mechanism in which the β-strands ($\beta 9$ and $\beta 10$) in the neck change conformation and peel off from the catalytic core has been suggested [112].

Either of these mechanisms, or more likely a combination of both, would make the 'arms' longer and thus make it easier for the unattached head to reach the next binding site. The tethered head would then be free to diffuse randomly in search of a new binding site, within the volume allowed by its tether; it will obviously be helpful if the search pattern is biased by a suitable tilting of the site to which the tether is attached. There is a problem reconciling the apparently fixed positions of the tethered head of kinesin observed by electron microscopy with this prediction of mobility, but we have suggested that it exchanges easily between parked and freely diffusing states [33].

It is not known whether other kinesin-related motors can also move in a hand-over-hand fashion. Differences in the structures of the necks of these motors should affect the processivity. Recent work shows that ncd and Eg5, a slow plus end-directed motor, are much less processive than kinesin [113]. In the case of kinesin, monomeric constructs have very low processivity [114–116]; apparently, a dimeric structure is required for a hand-over-hand mechanism to work. However, recent results show that a single molecule of Kif1A, which is monomeric in nature, can move along a microtubule processively [117]. These motors probably have evolved a different mechanism to slide along a microtubule without detaching.

Conclusion

For a motor domain moving along a polymeric track, the total distance moved in stepping from one binding site to the next is equal to the shift produced by the conformational change plus the distance diffused. The balance between the different contributions provided by diffusion and the power stroke will be different for different motor molecules. A combination of 3-D electron microscopy and X-ray crystallography has shown evidence for fairly substantial conformational changes in myosin molecules, which could largely explain the progress of myosin filaments along an F-actin track.

3-D electron microscopy has also shown that, although they move in opposite directions along microtubules, kinesin and ncd heads appear similar and bind in the same orientation to the same site on tubulin dimers. The tethered head of a dimeric kinesin molecule is oriented so that it could more easily reach the next site in the plus direction on the same protofilament, whereas the second ncd head points towards the next site in the minus direction (fig. 4b). However, the scale of the conformational change in an attached kinesin head, as observed in the presence of different nucleotides (fig. 4), seems small compared with the 16-nm distance that its partner must move between its successive binding sites. Thus, diffusion of the tethered head may play a substantial part in the processive stepping of kinesin.

Acknowledgements. We are indebted to Dr. Rob Cross for being a constant source of inspiring ideas, as well as for providing us with motor proteins expressed in his laboratory.

1 Stewart R. J., Thaler J. P. and Goldstein L. S. B. (1993) Direction of microtubule movement is an intrinsic property of the motor domains of kinesin heavy chain and *Drosophila* ncd protein. Proc. Natl. Acad. Sci. USA **90:** 5209–5213
2 Huang T. G. and Hackney D. D. (1994) *Drosophila* kinesin minimal motor domain expressed in *Escherichia-coli* – purification and kinetic characterization. J. Biol. Chem. **269:** 16493–16501
3 Holmes K. C. (1996) Muscle proteins – their actions and interctions. Curr. Opin. Struct. Biol. **6:** 781–789
4 Walker R. A., Salmon E. D. and Endow S. A. (1990) The *Drosophila* claret segregation protein is a minus-end directed motor molecule. Nature **347:** 780–782
5 McDonald H. B., Stewart R. J. and Goldstein L. S. B. (1990) The kinesin-like ncd protein of *Drosophila* is a minus end-directed microtubule motor. Cell **63:** 1159–1165
6 Hirose K., Lockhart A., Cross R. A. and Amos L. A. (1995) Nucleotide-dependent angular change in kinesin motor domain bound to tubulin. Nature (London) **376:** 277–279
7 Hoenger A., Sablin E. P., Vale R. D., Fletterick R. J. and Milligan R. A. (1995) Three-dimensional structure of a tubulin-motor-protein complex. Nature **376:** 271–274
8 Kikkawa M., Ishikawa T., Wakabayashi T. and Hirokawa N. (1995) Three-dimensional structure of the kinesin head-microtubule complex. Nature **376:** 274–279
9 Kull F. J., Sablin E. P., Lau R., Fletterick R. J. and Vale R. D. (1996) Crystal structure of the kinesin motor domain reveals a structural similarity to myosin. Nature **380:** 550–555
10 Sablin E. P., Kull F. J., Cooke R., Vale R. D. and Fletterick R. J. (1996) Crystal structure of the motor domain of the kinesin-related motor ncd. Nature **380:** 555–559
11 Hirokawa N. (1998) Kinesin and dynein superfamily proteins and the mechanism of organelle transport. Science **279:** 519–526
12 Chandra R., Salmon E. D., Erickson H. P., Lockhart A. and Endow S. A. (1993) Structural and functional domains of the *Drosophila* ncd microtubule motor protein. J. Biol. Chem. **268:** 9005–9013
13 Block S. M. (1998) Leading the procession: new insights into kinesin motors. J. Cell Biol. **140:** 1281–1284
14 Vale R. D. and Fletterick R. J. (1997) The design plan of kinesin motors. Annu. Rev. Cell Dev. Biol. **13:** 745–777
15 Inoue Y., Toyoshima Y. Y., Iwane A. H., Morimoto S., Higuchi H. and Yanagida T. (1997) Movement of truncated kinesin fragments with a short or an artificial flexible neck. Proc. Natl. Acad. Sci. USA **94:** 7275–7280
16 Sablin E., Case R. B., Dai S. C., Hart C. L., Ruby A., Vale R. D. et al. (1998) Direction determination in the minus-end-directed kinesin motor ncd. Nature **395:** 813–816
17 Hackney D. D. (1996) Myosin and kinesin – mother and child reunited. Chem. Biol. **3:** 525–528

18 Vale R. D. (1996) Switches, latches and amplifiers: common themes of G proteins and molecular motors. J. Cell Biol. **135:** 291–302
19 Bagshaw C. R. (1993) Muscle Contraction, Chapman Hill, New York
20 Howard J. (1996) The movement of kinesin along microtubules. Ann. Rev. Physiol. **58:** 703–729
21 Rayment I. and Smith C. (1996) The active site of myosin. Ann. Rev. Physiol. **58:** 671–702
22 Hackney D. D. (1996) The kinetic cycles of myosin, kinesin and dynein. Ann. Rev. Physiol. **58:** 731–750
23 Song Y.-H. and Mandelkow E. (1993) Recombinant kinesin motor domain binds to β-tubulin and decorates microtubules with a B surface lattice. Proc. Natl. Acad. Sci. USA **90:** 1671–1675
24 Harrison B. C., Marchese-Ragona S. P., Gilbert S. P., Cheng N., Steven A. C. and Johnson K. A. (1993) Decoration of the microtubule surface by one kinesin head per tubulin heterodimer. Nature **362:** 73–75
25 Song Y.-H. and Mandelkow E. (1995) The anatomy of flagellar microtubules: polarity, seam, junctions and lattice. J. Cell Biol. **128:** 81–94
26 Hirose K., Fan J. and Amos L. A. (1995) Re-examination of the polarity of microtubules and sheets decorated with kinesin motor domain. J. Mol. Biol. **251:** 329–333
27 Amos L. A. and Hirose K. (1997) The structure of microtubule-motor complexes. Curr. Opin. Cell Biol. **9:** 4–11
28 Hoenger A. and Milligan R. A. (1996) Polarity of 2-D and 3-D maps of tubulin sheets and motor decorated sheets. J. Mol. Biol. **263:** 114–119
29 Thormählen M., Marx A., Müller S. A., Song Y., Mandelkow E. M., Aebi U. et al. (1998) Interaction of monomeric and dimeric kinesin with microtubules. J. Mol. Biol. **275:** 795–809
30 Hirose K., Amos W. B., Lockhart A., Cross R. A. and Amos L. A. (1997) Three-dimensional cryoelectron microscopy of 16-protofilament microtubules: structure, polarity and interaction with motor protein. J. Struct. Biol. **118:** 140–148
31 Crevel I. M.-T., Lockhart A. and Cross R. A. (1996) Weak and strong states of kinesin and ncd. J. Mol. Biol. **257:** 66–76
32 Hirose K., Cross R. A. and Amos L. A. (1998) Nucleotide-dependent structural changes in dimeric ncd molecules complexed to microtubules. J. Mol. Biol. **278:** 389–400
33 Hirose K., Lockhart A., Cross R. A. and Amos L. A. (1996) Three-dimensional cryoelectron microscopy of dimeric kinesin and ncd motor domains on microtubules. Proc. Natl. Acad. Sci. USA **93:** 9539–9544
34 Arnal I., Metoz F., DeBonis S. and Wade R. H. (1996) Three-dimensional structure of functional motor proteins on microtubules. Curr. Biol. **6:** 1265–1270
35 Sosa H. and Milligan R. A. (1996) Three-dimensional structure of ncd-decorated microtubules obtained by a back-projection method. J. Mol. Biol. **260:** 743–755
36 Sosa H., Dias D. P., Hoenger A., Whittaker M., Wilson-Kubalek E., Sablin E. et al. (1997) A model for the microtubule-ncd motor protein complex obtained by cryo-electron microscopy and image analysis. Cell **90:** 217–224
37 Hoenger A. and Milligan R. A. (1997) Motor domains of kinesin and ncd interact with microtubule protofilaments with the same binding geometry. J. Mol. Biol. **265:** 553–564
38 Nogales E., Wolf S. and Downing K. H. (1998a) Structure of the ab tubulin dimer by electron crystallography. Nature **391:** 199–203
39 Ray S., Wolf S. G., Howard J. and Downing K. H. (1995) Kinesin does not support the motility of zinc-macrotubes. Cell Motil. Cytoskel. **30:** 146–152
40 Sosa H., Hoenger A. and Milligan R. A. (1997) Three different apporoaches for calculating the three-dimensional structure of microtubules decorated with kinesin motor domains. J. Struct. Biol. **118:** 149–158
41 Moore P. B., Huxley H. E. and DeRosier D. J. (1970) Three-dimensional reconstruction of F-actin, thin filaments and decorated thin filaments. J. Mol. Biol. **50:** 279–295
42 Taylor K. A. and Amos L. A. (1981) A new model for the geometry of the binding of myosin crossbridges to muscle thin filaments. J. Mol. Biol. **147:** 297–324
43 Toyoshima C. and Wakabayashi T. (1985) Three-dimensional image analysis of the complex of thin filaments and myosin molecules from skeletal muscle. V. Assignment of actin in the actin-tropomyosin-myosin subfragment-1 complex. J. Biochem. **97:** 245–263
44 Milligan R. A. and Flicker P. F. (1987) Structural relationships of actin, myosin, and tropomyosin revealed by cryo-electron microscopy. J. Cell Biol. **105:** 29–39
45 Jontes J. D., Wilson-Kubalek E. M. and Milligan R. A. (1995) A 32° tail swing in brush border myosin I on ADP release. Nature **378:** 751–753
46 Whittaker M., Wilson-Kubalek E. M., Smith J. E., Faust L., Milligan R. A. and Sweeney H. L. (1995) A 35-Å movement of smooth muscle myosin on ADP release. Nature **378:** 748–751
47 Wade R. H. and Chrétien D. (1993) Cryoelectron microscopy of microtubules. J. Struct. Biol. **110:** 1–27
48 Kikkawa M., Ishikawa T., Nakata T., Wakabayashi T. and Hirokawa N. (1994) Direct visualization of the microtubule lattice seam both in vitro and in vivo. J. Cell Biol. **127:** 1965–1971
49 Lanzavecchia S., Bellon P. L., Dallai R. and Afzelius B. A. (1994) Three dimensional reconstructions of accessory tubules observed in the sperm axonemes of two insect species. J. Struct. Biol. **113:** 225–237
50 Wade R. H., Horowitz R. and Milligan R. A. (1995) Toward understanding the structure and interactions of microtubules and motor proteins. Proteins – Structure Function and Genetics **23:** 502–509
51 Metoz F., Arnal I. and Wade R. H. (1997) Tomography without tilt: three-dimensional imaging of microtubule/motor complexes. J. Struct. Biol. **118:** 159–168
52 Ray S., Meyhöfer E., Milligan R. A. and Howard J. (1993) Kinesin follows the microtubule's protofilament axis. J. Cell Biol. **121:** 1083–1093
53 Hoenger A., Sack S., Thormählen M., Marx A., Müller J., Gross H. et al. (1998) Image reconstructions of microtubules decorated with monomeric and dimeric kinesins: comparison with x-ray structure and implications for motility. J. Cell Biol. **141:** 419–430
54 Walker R. A. (1995) Ncd and kinesin motor domains interact with both alpha-tubulin and beta-tubulin. Proc. Natl. Acad. Sci. USA **92:** 5960–5964
55 Tucker C. and Goldstein L. S. B. (1997) Probing the kinesin-microtubule interaction. J. Biol. Chem. **272:** 9481–9488
56 Larcher J. C., Boucher D., Lazereg S., Gros F. and Denoulet P. (1996) Interaction of kinesin motor domains with alpha- and beta-tubulin subunits at a tau-independent binding site. Regulation by polyglutamylation. J. Biol. Chem. **271:** 22117–22124
57 Jiang W., Stock M. F., Li X. and Hackney D. D. (1997) Influence of the kinesin neck domain on dimerization and ATPase kinetics. J. Biol. Chem. **272:** 7626–7632
58 Huang T. G., Suhan J. and Hackney D. D. (1994) *Drosophila* kinesin motor domain extending to amino-acid position-392 is dimeric when expressed in *Escherichia coli*. J. Biol. Chem. **269:** 16502–16507
59 Lockhart A., Crevel I. M.-T. C. and Cross R. A. (1995) Kinesin and ncd bind through a single head to microtubules and compete for a shared MT binding site. J. Mol. Biol. **249:** 763–771
60 Rayment I., Rypniewski W. R., Schmidt-Bäse K., Smith R., Tomchick D. R., Benning M. M. et al. (1993) Three-dimensional structure of myosin subfragment-1: a molecular motor. Science **261:** 50–58
61 Gulick A. M., Song H., Endow S. A. and Rayment I. (1998) X-ray crystal structure of the yeast Kar3 motor domain

complexed with Mg·ADP to 2.3 Å resolution. Biochemistry **37:** 1769–1776
62 Sack S., Müller J., Marx A., Thormählen M., Mandelkow E. M., Brady S. T. et al. (1997) X-ray structure of motor and neck domains from rat brain kinesin. Biochemistry **36:** 16155–16165
63 Kozielski F., Sack S., Marx A., Thormählen M., Schönbrunn E., Biou V. et al. (1997) The crystal structure of dimeric kinesin and implications for microtubule-dependent motility. Cell **91:** 985–994
64 Morii H., Takenawa T., Arisaka F. and Shimizu T. (1997) Identification of kinesin neck region as a stable α-helical coiled coil and its thermodynamic characterization. Biochemistry **36:** 1933–1942
65 Nogales E., Downing K. H., Amos L. A. and Löwe J. (1998b) Tubulin and FtsZ form a distinct family of GTPases. Nature Struct. Biol. **5:** 451–458
66 Kabsch W., Mannherz H. G., Suck D., Pai E. F. and Holmes K. C. (1990) Atomic structure of the actin: DNase I complex. Nature **347:** 37–44
67 McLaughlin P. J., Gooch J. T., Mannherz H.-G. and Weeds A. G. (1993) Structure of gelsolin segment 1-actin complex and the mechanism of filament severing. Nature **364:** 685–692
68 Schutt C. E., Myslik J. C., Rozycki M. D., Gooneesekere N. C. W. and Lindberg U. (1993) The structure of profilin: β-actin. Nature **365:** 810–816
69 Chik J. K., Lindberg U. and Schutt C. E. (1996) The structure of an open state of beta-actin at 2.65 angstrom resolution. J. Mol. Biol. **263:** 607–623
70 Holmes K. C., Popp D., Gebhard W. and Kabsch W. (1990) Atomic model of the actin filament. Nature **347:** 44–49
71 Lorenz M., Popp D. and Holmes K. C. (1993) Refinement of the F-actin model against X-ray fiber diffraction data by the use of a directed mutation algorithm. J. Mol. Biol. **234:** 826–836
72 Rayment I., Holden H. M., Whittaker M., Yohn C. B., Lorenz M., Holmes K. C. et al. (1993) Structure of the actin-myosin complex and its implications for muscle contraction. Science **261:** 58–65
73 Schroeder R. R., Manstein D. J., Holden J. W., Rayment I., Holmes K. C. and Spudich J. A. (1993) Three-dimensional atomic model of F-actin decorated with *Dictyostelium* myosin S1. Nature **364:** 171–174
74 Alonso M. C., Vanderkerckhove J. and Cross R. A. (1998) Proteolytic mapping of kinesin/ncd-microtubule interface: nucleotide-dependent conformational changes in the loops L8 and L12. EMBO J. **17:** 945–951
75 Woehlke G., Ruby A. K., Hart C. L., Ly B., Hom-Booher N. and Vale R. D. (1997) Microtubule interaction site of the kinesin motor. Cell **90:** 207–216
76 Yang J. T., Laymon R. A. and Goldstein L. S. B. (1989) A three-domain structure of kinesin heavy chain revealed by DNA sequence and microtubule binding analyses. Cell **56:** 879–889
77 Hirose K., Löwe J., Alonso M., Cross R. A. and Amos L. A. (1999) Congruent docking of dimeric kinesin and ncd into 3-d electron cryo-microscopy maps of microtubule-motor ADP complexes. Mol. Biol. Cell. **10:** 2063–2074
78 Kozielski F., Arnal I. and Wade R. H. (1998) A model of the microtubule–kinesin complex based on electron cryomicroscopy and X-ray crystallography. Curr. Biol. **8:** 191–198
79 Nogales E., Whittaker M., Milligan R. A. and Downing K. H. (1999) High resolution model of the microtubule. Cell **96:** 79–88
80 Reedy M. K., Holmes K. C. and Tregear R. T. (1965) Induced changes in orientation of the cross-bridge of glycerinated insect flight muscle. Nature **207:** 1276–1280
81 Jontes J. D. and Milligan R. A. (1997) Brush border myosin-I structure and ADP-dependent conformational changes revealed by cryoelectron microscopy and image analysis. J. Cell Biol. **139:** 683–693
82 Gollub J., Cremo C. R. and Cooke R. (1996) ADP release produces a rotation of the neck region of smooth myosin but not skeletal myosin. Nature Struct. Biol. **3:** 796–802
83 Fisher A. J., Smith C. A., Thoden J., Smith R., Sutoh K., Holden H. M. et al. (1995) X-ray structures of the myosin motor domain of *Dictyostelium discoideum* complexed with MgADPBeF(x) and MgADPAlF$_4$. Biochemistry **34:** 8960–8972
84 Smith C. A. and Rayment I. (1995) X-ray structure of the magnesium(II)-pyrophosphate complex of the truncated head of dictyostelium discoideum myosin to 2.7 Å resolution. Biochemistry **34:** 8973–8981
85 Smith C. A. and Rayment I. (1996) X-ray structure of the magnesium(II)·ADP·vanadate complex of the dictyostelium discoideum myosin motor domain to 1.9 Å resolution. Biochemistry **35:** 5404–5417
86 Gulick A. M., Bauer C. B., Thoden J. B. and Rayment I. (1997) X-ray structures of the MgADP, MgATPgS and MgAMPPNP complexes of the *Dictyostelium discoideum* myosin motor domain. Biochemistry **36:** 11619–11628
87 Holmes K. C. (1997) The swinging lever-arm hypothesis of muscle contraction. Curr. Biol. **7:** R112–R118
88 Gulick A. M. and Rayment I. (1997) Structural studies on myosin II: communication between distant protein domains. Bioessays **19:** 561–569
89 Holmes K. C. (1998) http://lala.mpimf-heidelberg.mpg.de/ ~ holmes/muscle/muscle2.html
90 Dominguez R., Freyzon Y., Trybus K. M. and Cohen C. (1998) Crystal structure of a vertebrate smooth muscle myosin motor domain and its complex with the essential light chain: visualization of the pre-power stroke state. Cell **94:** 559–571
91 Holmes K. C. (1998) A powerful stroke. Nature Struct. Biol. **5:** 940–942
92 Burke M. and Reisler E. (1977) Effect of nucleotide binding on the proximity of the essential sulfhydryl groups of mysin: chemical probing of movement of residues during conformational transitions. Biochemistry **16:** 5559–5563
93 Wells J. A. and Yount R. G. (1979) Active site trapping of nucleotides by crosslinking two sulfhydryls in myosin subfragment 1. Proc. Natl. Acad. Sci. USA **75:** 4966–4970
94 Suzuki Y., Yasunaga T., Ohkura R., Wakabayashi T. and Sutoh K. (1998) Swing of the lever arm of a myosin motor at the isomerization and phosphate-release steps. Nature **396:** 380–383
95 Uyeda T. Q. P., Abramson P. D. and Spudich J. A. (1996) The neck region of the myosin motor domain acts as a lever arm to generate movement. Pro. Natl. Acad. Sci. USA **93:** 4459–4464
96 Anson M., Geeves M. A., Kurzawa S. E. and Manstein D. J. (1996) Myosin motors with artificial lever arms. EMBO J. **15:** 6069–6074
97 Ishijima A., Kojima H., Funatsu T., Tokunaga M., Higuchi H., Tanaka H. et al. (1998) Simultaneous observation of individual ATPase and mechanical events by a single myosin molecule during interaction with actin. Cell **92:** 161–171
98 Kitamura K., Tokunaga M., Iwane A. H. and Yanagida T. (1999) A single myosin head moves along an actin filament with regular steps of 5.3 nanometres. Nature **397:** 129–134
99 Molloy J. E., Burns J. E., Kendrick-Jones J., Tregear R. T. and White D. C. S. (1995) Movement and force produced by a single myosin head. Nature **378:** 209–212
100 Guilford W. H., Dupuis D. E., Kennedy G., Wu J., Patlak J. B. and Warshaw D. M. (1997) Smooth muscle and skeletal muscle myosin produce similar unitary forces and displacements in the laser trap. Biophys. J. **72:** 1006–1021
101 Marx A., Thormählen M., Müller J., Sack S., Mandelkow E.-M. and Mandelkow E. (1998) Conformations of kinesin: solution vs. crystal structures and interactions with microtubules. Eur. Biophys. J. **27:** 455–465
102 Henningsen U. and Schliwa M. (1997) Reversal of the direction of movement of a molecular motor. Nature **389:** 93–96

103 Case R. B., Pierce D. W., Hom-Booher N., Hart C. L. and Vale R. D. (1997) The directional preference of kinesin motors is specified by an element outside of the motor catalytic domain. Cell **90:** 959–966
104 Endow S. A. and Waligora W. W. (1998) Determinants of kinesin motor polarity. Science **281:** 1200–1202
105 Greene E. A., Henikoff S. and Endow S. A. (1996) http://blocks.fhcrc.org/ ~ kinesin/
106 Block S. M. (1998) Kinesin: what gives? Cell **93:** 5–8
107 Hackney D. D. (1994) Evidence for alternating head catalysis by kinesin during microtubule-stimulated ATP hydrolysis. Proc. Natl. Acad. Sci. USA **91:** 6865–6869
108 Gilbert S. P., Moyer M. L. and Johnson K. A. (1998) Alternating site mechanism of the kinesin ATPase. Biochemistry **37:** 792–799
109 Svoboda K., Schmidt C. F., Schnapp B. J. and Block S. M. (1993) Direct observation of kinesin stepping by optical trapping interferometry. Nature **365:** 721–727
110 Tripet B., Vale R. D. and Hodges R. S. (1997) Demonstration of coiled-coil interactions within the kinesin neck region using synthetic peptides. J. Biol. Chem. **272:** 8946–8956
111 Thormählen M., Marx A., Sack S. and Mandelkow E. (1998) The coiled-coil helix in the neck of kinesin. J. Struct. Biol. **122:** 30–41
112 Romberg L., Pierce D. W. and Vale R. D. (1998) Role of the kinesin neck region in processive microtubule-based motility. J. Cell Biol. **140:** 1407–1416
113 Crevel I. M.-T. C., Lockhart A. and Cross R. A. (1997) Kinetic evidence for low chemical processivity in ncd and Eg5. J. Mol. Biol. **273:** 160–170
114 Hancock W. O. and Howard J. (1998) Processivity of the motor protein kinesin requires two heads. J. Cell Biol. **140:** 1395–1405
115 Young E. C., Mahtani H. K. and Gelles J. (1998) One-headed kinesin derivatives move by a non-processive, low-duty ratio mechanism unlike that of two-headed kinesin. Biochemistry **37:** 3467–3479
116 Vale R. D., Funatsu T., Pierce D. W., Romberg L., Harada Y. and Yanagida T. (1996) Direct observation of single kinesin molecules moving along microtubules. Nature **380:** 451–453
117 Okada Y. and Hirokawa N. (1999) A processive single-headed motor: kinesin superfamily protein KIF 1A. Science **283:** 1152–1157